TEM and DSC studies on the synthetic diamond grown from Fe–Ni–C–B system under HPHT

J.-H. GONG*, M.-S. LI
College of Materials Science and Engineering, Shandong University, Ji'nan 250061, People's Republic of China

B. XU
Department of Materials Science and Engineering, Shandong Institute of Architecture and Engineering, Ji'nan 250014, People's Republic of China

L.-W. YIN, Y.-X. LIU, H.-G. LIU
College of Materials Science and Engineering, Shandong University, Ji'nan 250061, People's Republic of China

Diamond was synthesized by the static pressure catalyst method may contain many kinds of impurities [1], which can affect the color, hardness, strength, thermal conductivity, optical absorption, and other physical properties of diamonds [2]. Evergrowing requirements imposed on thermal management materials in applications such as microelectronics; optical communications and semiconductor processing equipment drive the development of new materials with enhanced thermal conductivity [3]. The boron and nitrogen were two important impurities that could control the electronic properties of diamond through playing roles of donor and acceptor [4]. The reports on boron in the synthetic diamond grown at high-pressure high-temperature (HPHT) has not been found compared to that on nitrogen, which was ever studied extensively [5, 6]. Besides the effect on the electronic resistance of diamond, born could influence the outset temperature of oxidation resistance, i.e., the thermal stability of diamond crystals [7]. Further studies of the boron effect on thermal stability of diamond would have great significance in mechanical industry. In present paper, investigation was focused on both the microstructure and chemical composition of boron compounds in the diamond and their influence on the thermal stability of diamond crystals synthesized using Fe–Ni–B metal catalyst under HPHT conditions. In addition, we examined the effect of boron compounds on the outset temperature of oxidation resistance of synthetic diamond grown using boron-contained catalyst by different scanning calorimetry (DSC) techniques.

Four alloys: Fe–Ni, Fe–Ni–0.01wt%B, Fe–Ni–0.1 wt%B and Fe–Ni–0.4 wt%B, sampled as A, B, C, and D, respectively, were used as metal catalysts. They were placed alternately with graphite discs (purity 99.9%) to synthesize four types of boron-content diamond. In order to eliminate possible effects of adsorbed gases and water on the diamond synthesis, the raw materials were heat-treated at 1350 °C for about 2–3 hr in vacuum [8, 9]. The high-pressure high-temperature experiment was carried out in a cubic anvil apparatus. This cell assembly was brought up to pressure of 5.3 GPa by a modified belt-type high-pressure apparatus and then heated to a temperature of about 1570 K. After keeping the sample at this temperature for 8 min, the temperature was decreased rapidly by turning off the electric power. The samples were broke and diamond crystals were recovered by dissolving the metals and the residual graphite in a boiling mixture of H_2SO_4 and HNO_3 acids, followed by extensive washing. Some HPHT grown diamond crystals of about 0.5 mm in dimension was first mechanically polished. After that, it was ground by ion beam milling till it was suitable for TEM observation. For these studies, a Philips CM-30 type of transmission electron microscope equipped with an EDAX energy dispersive X-ray spectrometer (EDS) system was used. EDS was used in combination with selected area electron diffraction (SAD) to examine the composition and the crystal structure of the inclusions in the synthetic diamond grown from Fe–Ni–C–B system.

The four types of diamonds with different boron content were thermally characterized by differential scanning calorimetry (DSC) in DSC-404C equipment. All the experiments were accomplished up to 1000 °C at a constant heating rate of 20 °C/min in air.

The TEM investigation on the impurities in the synthetic diamond grown from Fe–Ni–C system has ever been reported in literatures [10–12]. Compared to those results, we found some new boride compounds in the boron-contained diamond grown from Fe–Ni–B–C system. Fig. 1a shows a TEM image of a kind of boride inclusion in the synthetic. The Fe and Ni elements can be

---

* Author to whom all correspondence should be addressed.

0022-2461
DOI: 10.1007/s10853-006-6338-9

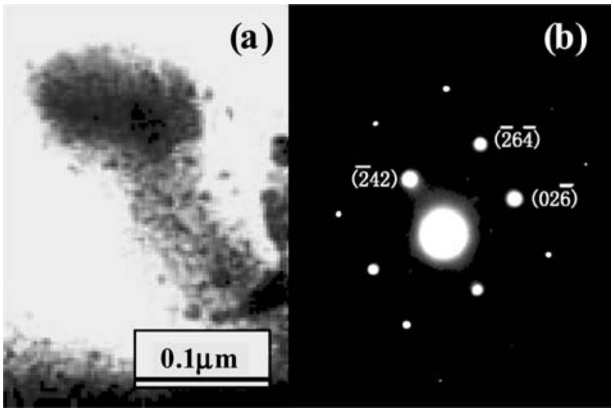

Figure 1 (a) TEM image of fcc $(FeNi)_{23}(CB)_6$ inclusion in a diamond. (b) Corresponding SAD pattern of the $(FeNi)_{23}(CB)_6$ from zone axis of [731].

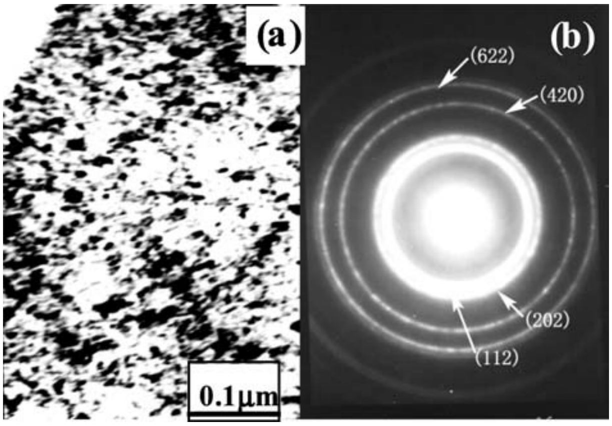

Figure 2 (a) TEM image of polycrystalline $(FeNi)_3$ (CB) inclusion. (b) Corresponding SAD pattern of the $(FeNi)_3(CB)$.

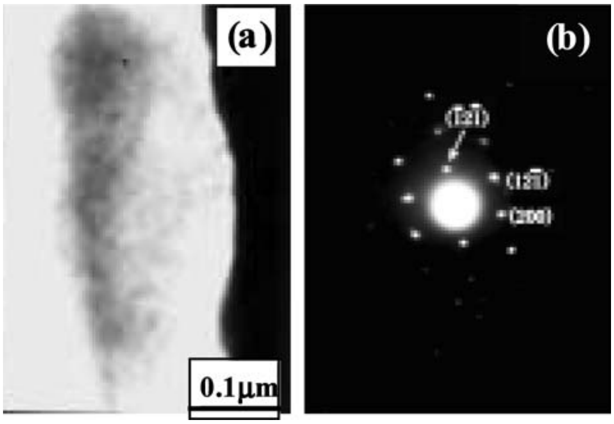

Figure 3 (a) TEM image of T (Fe, Ni) B layer inclusion in a diamond; (b) Corresponding SAD pattern from the zone axis of [012] determines it is orthorhombic.

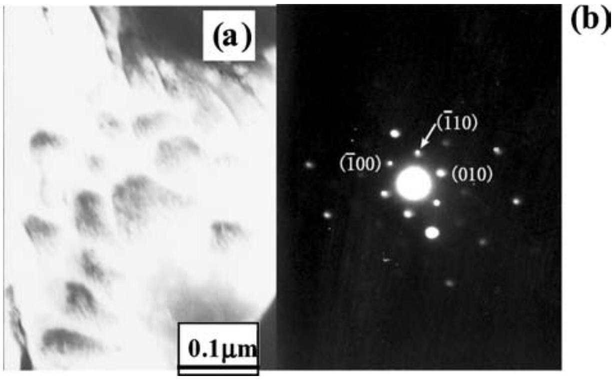

Figure 4 (a) TEM image of hexagonal B_4C inclusion in a diamond; (b) Corresponding SAD pattern of the B_4C phase from the zone axis of [211].

detected from the EDS analysis of the metallic inclusion. It is determined that the inclusion is f.c.c. $(Fe, Ni)_{23}(CB)_6$ by the identification of corresponding selected area electron diffraction (SAD) pattern from the [731] zone axis of the metallic inclusion, as shown in Fig. 1b.

Fig. 2a illustrates the TEM image of polycrystalline $(Fe, Ni)_3$ (C, B) in the diamond. EDS analysis of this phase suggests the existence of iron and nickel. Fig. 2(b) is the corresponding SAD ring indicates that it is the orthorhombic $(Fe, Ni)_3(C, B)$. Pavel ever confirmed the Fe_3C presence as main phase of metallic inclusions in diamond crystals grown in Fe–C system and the $(FeNi)_3C$ presence in synthetic diamond crystals grown in Fe–Ni–C systems [13, 14]. The formation of $(Fe, Ni)_{23}(CB)_6$ and $(Fe, Ni)_3(C, B)$ can be consulted to that of the $(Fe, Ni)_{23}C_6$ and $(Fe, Ni)_3C$, which was described in literature [15, 16]. It is inclined to think that $(Fe, Ni)_7C_3$ formed under a pressure ranging from 4.7 to 6 GPa during the process of the diamond crystal growth, when iron and nickel reacted with graphite trapped in the diamond, firstly, $(Fe, Ni)_7C_3$ appears as a metastable phase (900–1050 °C), and then it transforms into a more stable phase $(Fe, Ni)_{23}C_6$ and $(Fe, Ni)_3C$ as the temperature decreased. The microstructure, characterization, thermal and magnetic properties of the $(Fe, Ni)_3C$ have been studied by various extensively techniques [17, 18]. For similar atom radius, boron atoms are easy to take place of carbon atoms of carbide and then $(Fe, Ni)_{23}(C, B)_6$ and $(Fe, Ni)_3(C, B)$ are formed. They are remained as inclusions in the diamond crystals during the course of sharp quenching process.

Another boride impurity trapped in the diamond is shown in Fig. 3. EDS analysis demonstrates the existence of iron and nickel, further studies of the corresponding SAD pattern of the inclusion from [211] zone axis indicated that this inclusion is the orthorhombic (Fe, Ni)B phase, shown in Fig. 3b. Fig. 3a shows the TEM image of (Fe, Ni)B layer.

Fig. 4 shows boron carbide contained in the diamond crystal. It can be identified from the corresponding electron diffraction pattern of [211] zone axis illustrated in Fig. 4b. The boron atoms diffused into diamond from molten alloy catalyst. And boron diffusion into diamond lattice was studied in [19]. Boron concentration fluctuated under the influence of temperature and pressure and has more concentration than carbon atoms at some local area. Interparticle collision and coalescence of carbon and boron atoms resulted in the formation of B_4C. Within the temperature range 1000–1100 °C $Fe–B_4C$ would

TABLE I Thermal stability of diamonds grown from different boron-contained catalyst

Sample	A	B	C	D
Catalyst composition	Fe–Ni	Fe–Ni–0.01 wt%B	Fe–Ni–0.2 wt%B	Fe–Ni–0.4 wt%B
Outset temperature (°C)	761.7	881.6	928.9	829.7

decompose into a mixture of $Fe_3(C, B)$ crystals and graphite with relatively high microhardness in the place of initial particles of B_4C according to the constitutional diagram of the Fe–B–C [20].

Differential scanning calorimetric curves (DSC) of the diamonds grown from sample A, B, C, and D alloy catalysts were presented in Fig. 5 with the downward direction indicating an exothermic process. Under the temperature of 600 °C, all samples possess similar thermal characters with no obvious endothermic or exothermic process. Increasing the temperature further, diamonds began to oxidize at different temperature for the interaction of $C + O_2 \rightarrow CO_2 + Q$ present. Table I reports the experimental data obtained by DSC techniques at a heating rate of 20 °C/min. The diamond grown from sample A catalyst oxidized firstly at 761.7 °C, and the diamond from sample B delayed to oxidize at 881.6 °C. It is noticed that the diamonds grown from sample C has the highest outset temperatures of the oxidation resistance, which is 167.2 °C higher than that of the diamond from Fe–Ni alloy catalyst. Such improvement is an exciting result for cutting industry. But the outset oxidation temperature of the diamond from sample D, i.e. Fe–Ni–2 wt%B, decreased rapidly while that is still higher than that of the non boron diamond. Therefore the thermal stability of diamond increases originally and decreases subsequently with boron content from 0.01 to 0.4 wt% in alloy catalyst. This means different boron content in the catalyst is an important factor that affects the oxidation resistance of diamond differently.

In fact the different boron content results in various boride compounds concentration in the synthetic diamond. It is known that the higher the boron concentration in Fe–B rapidly solidified alloys the higher the thermal stability becomes [21]. B_4C was demonstrated as an effective compounds to enhance the thermal stability of coatings [22]. It has been reported that the rise in resistance to oxidation of CSPD with the addition of boron compounds to an initial alloy is caused by the formation of amorphous boron oxide B_2O_3 as a result of interaction of the boron compound with oxygen from the air [23]. And the resistance to oxidation of sintered polycrystalin diamond raised is also connected with formation of the B_2O_3 protective film [24]. The effect mechanism of $(FeNi)_{23}(CB)_6$ and $(Fe, Ni)_3(C, B)$ on the crystal structure and thermal stability of diamonds needs further studies.

1. Diamonds grown from Fe–Ni–B catalyst under HPHT includes various boride compounds, such as f.-c.-c-. $(Fe, Ni)_{23}(CB)_6$, polycrystalline $(FeNi)_3$ (CB), orthorhombic (Fe, Ni)B and hexagonal B_4C.

2. Thermal stability of the diamond from different Fe–Ni–B alloy catalysts studied strongly depends on boron concentration of the catalysts. The increase of boron content from 0.01 to 0.4 wt% resulted in the outset temperature to oxidation resistance of diamonds

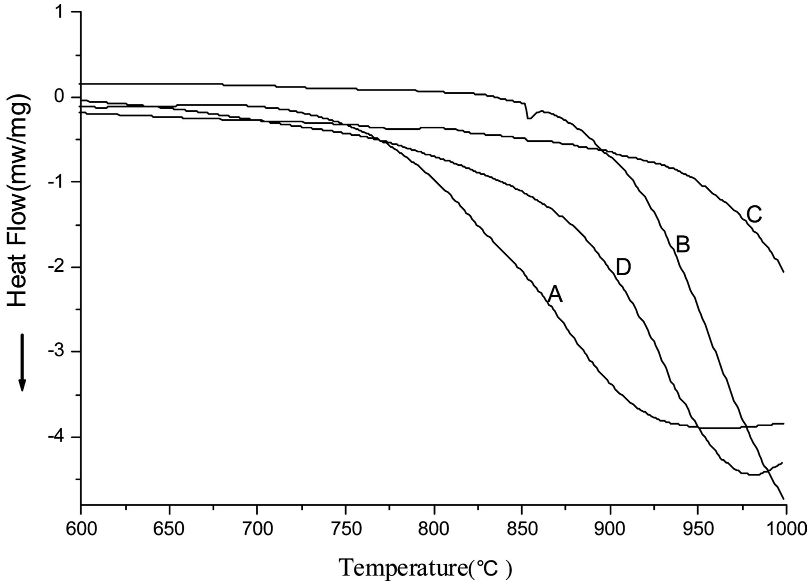

Figure 5 DSC curves of the diamonds grown from catalyst with different B content: A-0 wt%; B-0.01 wt%; C-0.2 wt%; D-0.4 wt% at heating rate of 20 °C/min. Downward direction indicates an exothermic process.

increases originally and decreases subsequently. The highest outset oxidation temperature is 928.9 °C caused by Fe–Ni–0.2 wt%B catalyst, which is 120 K higher than that of the non boron diamonds.

3. It is the boron compounds included in the diamond crystals that affect the thermal stability of synthetic diamonds. The mechanism needs further studies and that would improve cutting industry significantly.

Acknowledgments

This work was supported by the National Natural Foundation of China (Grant No. 50372035 and No. 50371048)

References

1. C. M. HUGGINS and P. CANNON, *Nature* **120** (1961) 829.
2. Appendix B, “Properties of Natural and Synthetic Diamond” (Academic Press, London, 1992).
3. K. WATARI and S. L. SHINDE, *High thermal conductivity materials MRS Bull.* **26**(6) (2001) 440–441.
4. KANEKO JUNICHI, YONEZAWA CHUSHIRO and KASUQAI YOSHIMI, *Diamond Related Mater.* **9** (2000) 2019–2023.
5. F. V. KAMINSKY and G. K. KHACHATRYAN, *Can. Mineral.* **39** (2001) 1733–1745.
6. S. A. KAJIHARA, A. ANTONELLI and J. BERNHOLC, *Physica B: Condens. Matter* **185** (1993) 144–149.
7. QI LIANGQ, S. A. CATLEDQE and A. VOHRA, Materials Research Society Symposium-Proceedings, v 791, Mechanical Properties of Nanostructured Materials and Nonocomposites, (2003) pp. 265–270.
8. J.-Y. CHOI, Y.-E. YONG and J.-S. KIM, *Diamond Related Mater.* **7**(8) (1998) 1196–1200.
9. H. SHIN-ICHI, S. KAZUZKI and N. SHIQEHARU, *J. Mater. Sci.* **17**(7) (1982) 1856–1862.
10. L.-W. YIN, Z.-D. ZOU and M.-W. LI, *Microstructure and Processing,* **293** (1) (2000) 107–111.
11. L.-W. YIN, Z.-D. ZOU and M.-S. LI, *Diamond Related Mater.,* **9** (12) (2000) 2006–2009.
12. L.-W. YIN, M.-S. LI and Y.-X. LIU, *J. Mater. Sci. Lett* **19**(22) (2000) 2001–2002.
13. E. PAVEL, Gh. BALUTA and D. BARB, *Solid State Commun.* **76** (1990) 531–533.
14. E. PAVEL, G. H. BALUTA and D. BARB, *Mater. Lett.* **10** (1990) 62–65.
15. L. W. YIN, Z. D. ZOU and M. S. LI, *J. Cryst. Growth* **218** (2000) 455–458.
16. Y. A. KOCHERZHINSKII, O. G. KULIK and V. Z. TURKEVICH, *High Temp.-High Press* **25** (1993) 113.
17. E. PAVEL, Gh. BALUTA and D. BARB, *J. Mater. Sci.* **28** (1993) 1645–1647.
18. E. PAVEL, Gh. BALUTA and C. GIURQIU, *Mater. Sci. Eng. A* Structural Materials: Properties, Microstructure and Processing, **A150**, 1992: L9-L10.
19. T. SUNG, G. POPOVICI and M. A. PRELAS, *Diamonds Electron. Appl.* (1995).
20. YU. V. TUROV, B. M. KHUSID and L. VOROSHNIN, *Poroshkovaya Metallurgiya* **6** (1991) 25–31.
21. J. J. SUÑOL, A. GONZÁLEZ and J. SAURINA, *Mater. Sci. Eng. A* **375–377**(15) (2004) 874-880.
22. P. MOGILEVSKY, I. GOTMAN and E. Y. GUTMANAS **171** (1) (1993) 271–279.
23. V. P. POLIAKOV, A. A. ERMOLAEV and A. I. LAPTEV, *Diamond Related Mater.* **10**(11) (2001) 2024–2029.
24. V. V. LOPAREV, A. M. VEPRINTSEV and A. M. MANUHIN, *Sverhtverdye Materially* **6** (1984) 11–14.

Received 16 November 2004
and accepted 8 September 2005